RSC Advances

ROYAL SOCIETY OF CHEMISTRY

www.rsc.org/advances

Cite this: DOI: 10.1039/c0xx00000x

www.rsc.org/xxxxxx

ARTICLE TYPE

Synthesis and evaluation of cationically modified poly (styrene –alt-maleic anhydride) nanocarriers for intracellular gene delivery

Aji Alex M.R,[a,b] Neha Nagpal,[c] Ritu Kulshreshtha [c] and Veena Koul[*a,b]

Received (in XXX, XXX) Xth XXXXXXXXX 20XX, Accepted Xth XXXXXXXXX 20XX

DOI: 10.1039/b000000x

Intracellular gene delivery properties of styrene-alt-maleic anhydride based graft co-polymers embedded with various cationic moieties were analyzed. Quaternary nitrogen units were grafted to the polymer via aromatic (quaternized isonicotinic acid), aliphatic (glycidyl trimethyl ammonium chloride) and cyclo aliphatic (quaternized piperazine) molecules. Primary/secondary amine-grafted polymers were obtained by conjugating L-arginine and spermine. These amphiphilic graft copolymers readily formed core shell type nanoparticles of size < 100 nm. Cytotoxicity, haemo-compatibility, endosomal rupturing property, polyplex formation and resistance to DNase degradation were evaluated for all the polymeric derivatives, and found to have a strong correlation with the nature of cationic moieties. Cytotoxic potential of cations were in the order; quaternized piperazine > spermine > quaternized isonicotinic acid, L-arginine and glycidyl trimethyl ammonium chloride. Excellent endosomal rupturing efficiency (% haemolysis at pH 5.5) was observed for quaternized isonicotinic acid (~ 86 %), spermine (~ 78 %) and L-arginine (~ 73 %) grafts. Polyplexes of quaternized derivatives showed reduced DNase resistance probably due to electrostatic repulsion of carboxylic side chains. L-arginine and spermine grafted nanocarriers exhibited efficient DNA complexation and DNase resistance, and hence were evaluated for transfection efficiency in MCF-7 cells. Spermine graft depicted 1.45 fold higher transfection efficiency than the positive control (branched polyethyleneimine, 25,000 KDa), and L-arginine graft achieved comparable efficiency to that of the control. These amphiphilic nanocarriers depicts promising potential for *in vivo* gene delivery applications due to their lower cytotoxicity, pH responsiveness, large scale production feasibility and ease of chemical modification.

Introduction

Gene therapy using non viral vectors has gained clinical significance due to its myriad application in treating various diseases, especially cancer. In this context, lipid and polymer based carriers depicted their potential for intracellular gene disposition by overcoming physicochemical and cellular barriers.[1] In most of the gene delivery approaches, either lipid or the polymeric carriers have been formulated in to their respective nanoparticles for achieving long circulation half life, gene complexation efficiency and low toxicity. The polymeric vectors have advantages over lipid vectors due to improved stability, enhanced water solubility, ease of chemical modification for targeted delivery etc.[2] Here in, we present the design, synthesis and gene delivery application of low molecular weight poly (styrene –alt-maleic anhydride) (PSMA) grafts. PSMA is a co-polymer which provides ample opportunities for functionalization due to the presence of maleic anhydride groups.[3] Ring opening of maleic anhydride units impart amphiphilic nature to PSMA, thus promoting its self assembly in aqueous media. [4] Protonation of the carboxylate ions of this amphiphilic polymer, at endosomal pH, triggers the conversion of a hydrophilic and biologically inert state to hydrophobic state.[5] In this protonated state, PSMA can destabilize the endosomal membrane facilitating the delivery of incorporated bioactive molecules to cytosol. This pH responsive behaviour of PSMA makes it an excellent carrier for intracellular delivery.

Clinical applications of PSMA have been well studied and reported.[6-10] Various polymeric prodrugs have been prepared using PSMA with enhanced physicochemical, pharmacokinetic and pharmacodynamic properties. Low molecular weight (< 6 KDa) PSMA has been successfully employed to deliver neocarzinostatin, an antitumor protein.[6] The protein –polymer conjugate exhibited enhanced lipid solubility and achieved 10 fold increase in the plasma half life of neocarzinostatin. This protein conjugate has been launched in market as an effective treatment for hepatocellular carcinoma, under the commercial name *zinostatin,* which has shown 70-90 % success rate in treated patients.[7] Various other anticancer drugs have also been successfully conjugated to PSMA and studied. Antitumor activities of drugs like doxorubicin[8], pirarubicin[9], YIGSR[10] (a sequence present in laminin) etc. have shown to be significantly

improved after incorporating in to PSMA. PSMA conjugates were shown to promote immunopotentiation in host cells by activating macrophages, T cells, interferons etc. They also form a non covalent binding with albumin during circulation, which in turn decreases their systemic clearance.[11] Alkylamine derivatives of PSMA have shown enormous potential for intracellular drug delivery due to their pH responsive behavior.[12]

Although PSMA has been widely investigated for drug delivery, its application in gene delivery is still a less exploited area.[13] In the present study, various possibilities of utilizing PSMA for efficient gene delivery were explored. For this purpose, we have embedded the polymer with quaternary ammonium cations via aromatic (isonicotinic acid), aliphatic (glycidyl trimethylammonium chloride) and cyclo aliphatic (1-(2-aminoethyl) piperazine) compounds. Isonicotinic acid is a highly biocompatible aromatic compound. Isoniazid, an effective drug in the treatment of tuberculosis, has been derivatized from isonicotinic acid.[14] The conjugation of isonicotinic acid to antimicrobial silver coordination compounds resulted in their improved biocompatibility.[15] Glycidyl trimethyl ammonium chloride is an aliphatic compound, with epoxy ring at one end and quaternary nitrogen at the other end. It's application as a DNA complexing agent has been well established.[16] 1-(2-aminoethyl) piperazine, a cyclo aliphatic compound, has been experimentally reported to enhance the gene delivery efficiency of various carriers.[17-19] In addition, commonly employed and efficient transfecting molecules such as L-arginine[20-22] and spermine[23-25] were also conjugated to PSMA. L-arginine and spermine are highly biocompatible endogenous molecules present in the physiological system. They have the ability to complex and condense genetic materials through electrostatic interactions.[26] The synthesized amphiphilic polymeric derivatives were characterized using ^{1}H-NMR and FT-IR, and evaluated for their cytotoxicity, haemocompatibility, endosomal rupturing property, polyplex formation and resistance against DNase I degradation.

Experimental Part

Materials

PSMA with a styrene to maleic anhydride molar ratio of 2:1 (molecular weight 7500 Da) was obtained from Sartomer Company Inc (Quarry bay, Hong Kong). 3-amino-1-propanol, Di-tert-butyl dicarbonate, 1-(2-aminoethyl)piperazine, dicyclohexyl carbodiimide (DCC), N-hydroxy succinimide, spermine, glycidyl trimethyl ammonium chloride, Boc-Arginine(Mts)-OH cyclohexylammonium salt, trifluoromethanesulfonicacid, thioanisole, bovine serum albumin (molecular weight 66 KDa), 3-(4,5-dimethylthiazol-2-yl)-2,5-diphenyltetrazolium bromide(MTT), branched polyethyleneimine (PEI) (average molecular weight 25,000 KDa), DNase I and ethidium bromide were purchased from Sigma-Aldrich (Bangalore, India). Trypsin-ethylenediamine tetra acetic acid, Dulbeccos modified eagles media (DMEM), penicillin/streptomycin antibiotic solution, fetal bovine serum and agarose were purchased from Himedia (India). 1-ethyl-3-(3-dimethylaminopropyl) carbodiimide hydrochloride (EDC. HCl), isonicotinic acid, trifluoroacetic acid, phenol and triethyl amine (NEt_3) were obtained from Merck millipore (India). DsRed-Express-N1 plasmid vector (4.7 Kb) was obtained from Clontech laboratories, Inc (USA). All other solvents and reagents used were of analytical grade. Purified water obtained from MilliQ Plus (Millipore) was used during experiments.

Grafting of PSMA with quaternized isonicotinic acid

Isonicotinic acid was converted in to 3-aminopropyl isonicotinate (ESI† S.1), and grafted to PSMA. Briefly, 0.3 g PSMA (approx. 0.98 mM of monomer units) was added to dichloromethane (15 mL) containing 3-aminopropyl isonicotinate (0.55 g, 1.85 mM) and triethylamine (NEt_3) (0.2g, 2mM). The reaction was carried out for overnight at room temperature, and the solvent was then removed using rotary flash evaporator. The obtained polymeric derivative was purified by washing with acidic water (pH 5) followed by dichloromethane. The purified product was then quaternized by reacting with methyl iodide (2 mol equivalent), using dimethyl sulfoxide as solvent, for 24 hrs. The solvent was then removed under high vacuum (Hind Hivac, India), and the quaternized derivative was purified by washing successively with water and dichloromethane.

Synthesis of quaternized piperazine grafted PSMA

1-(2-aminoethyl) piperazine (1g, 7.7 mM) and PSMA (1.18 g, 3.85 mM) were reacted in DMF (15 mL), for 12 hours, at room temperature. After the completion of reaction, the precipitated product was filtered, and the crude product was washed with tetrahydrofuran followed by acetone. Quaternization of the polymeric derivative was done by reacting with methyl iodide (4 mol equivalent) in DMSO, for 24 hrs, at room temperature (scheme II). The obtained product was precipitated by adding ethyl acetate to the reaction mixture, and purified by washing with methanol followed by evaporating under high vacuum.

Synthesis of glycidyl trimethyl ammonium chloride grafted PSMA

PSMA was grafted with 3-amino-1-propanol through esterification (ESI† S.2). In the next step, glycidyl trimethyl ammonium chloride was coupled to the free amino groups of PSMA grafted with 3-amino-1-propanol. Briefly, PSMA conjugated with 3-amino-1-propanol (0.5 g, 1.3 mM) was dispersed in 5 % NaOH solution (15 mL) followed by the addition of glycidyl trimethylammonium chloride (0.4 g, 2.6 mM), and reaction was carried out at 80° Celsius for 24 hours (scheme III). The reaction mixture was then acidified to pH 2 by adding 0.1 N HCl, in order to precipitate the product, and then the product was purified by washing repeatedly with milliQ water.

Grafting of L-arginine to PSMA

Boc-Arginine (Mts)-OH cyclohexylammonium salt (0.6 g, 1.07 mM) was desalted (as per manufacturers protocol) and activated with N-hydroxy succinimide (0.108 g, 0.94 mM) and DCC (0.194 g, 0.94 mM), in dimethyl formamide (10 mL), at room temperature for overnight. The precipitated by product was removed by filtration and the filtrate was collected. The collected filtrate was slowly added to DMF (10 mL) containing PSMA grafted with 3-amino-1-propanol (0.25g, 0.65 mM) and NEt_3 (0.13 g, 1.3 mM), and the reaction was carried out under continuous stirring for 12 hours (Scheme IV). After the completion of reaction, solvent was removed under high vacuum

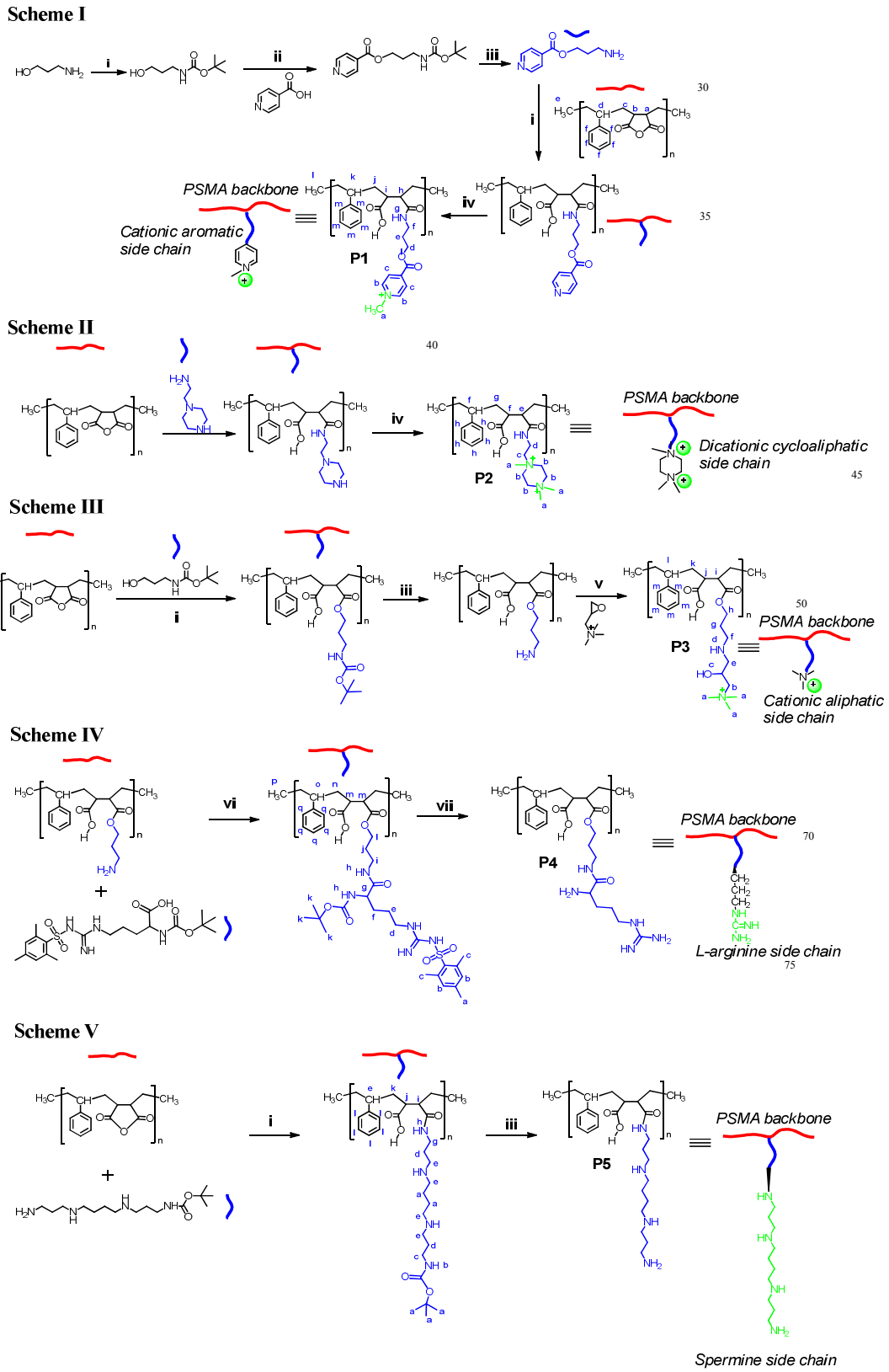

Figure 1. Schematic representation of the synthesis of various PSMA derivatives. (i) NEt_3 ,RT,12 h (dry CH_2Cl_2) (ii) EDC/NHS, NEt_3, 0 ºC - RT, 12 h (iii) TFA- CH_2Cl_2 ,RT, 3 h (iv) CH_3I , $(CH_3)_2SO$, RT, 24 h (v) 5 % NaOH, 80 ºC, 24 h (vi) DCC/NHS, NEt_3 , 0 ºC – RT, 12 h (vii) TFA: Phenol : H_2O: triisoprpylsilane: thioanisole : EDT (82.5:5:5:5:1:1.5), RT, 3 h.

and the residue was washed with acidic water (pH 5) followed by dichloromethane. Boc and mesitylene-2-sulfonyl groups in the obtained polymeric derivative were removed by treating with cleavage cocktail viz. tifluoroacetic acid: phenol: triisopropylsilane : water: thioanisole: ethylenedithiol (EDT), in the ratio 82.5 : 5:5: 5: 1: 1.5, for 3 h, at room temperature. The resulting product was dried by evaporating the solvents under high vacuum, and purified by washing successively with n-hexane and acetone.

Synthesis of spermine grafted PSMA

Mono- N-Boc protected spermine was synthesized by reacting spermine with Boc anhydride (ESI† S.3). PSMA (0.125 g, 0.4 mM) was treated with mono N-Boc spermine (0.247 g, 0.8 mM), in the presence of NEt_3 (0.04 g, 0.4 mM), using dry DMF (10 mL) as solvent (Scheme V). In the final step, Boc was removed from the polymer by treating with TFA: DCM mixture (1:1) for 3 hours. The spermine grafted PSMA was then purified by washing repeatedly with water.

All the intermediate compounds in the synthesis and final products were suitably characterized using ^{1}H NMR (300 MHz, Brukers, USA) and ATR –FTIR (PerkinElmer, USA). For convenience, the co polymeric grafts of PSMA with quaternized isonicotinic, quaternized piperazine, glycidyl trimethyl ammonium chloride, L-arginine and spermine are abbreviated as **P1**, **P2**, **P3**, **P4** and **P5** respectively.

Formulation of nanoparticles

Nanoparticles of PSMA derivatives were formulated using nanoprecipitation method. During formulation, weight of all the polymeric derivatives was fixed at 2 mg. Quaternized polymeric derivatives viz. **P1** and **P3** and L-arginine grafted PSMA (**P4**) were weighed and dissolved in 0.1 mL of DMSO. The DMSO solution was then mixed with milliQ water (4.9 mL) under stirring at 400 rpm. The polymeric particles were then subjected to probe sonication, at 100 W, for suitable time. Quaternized piperazine grafted PSMA (**P2**) nanoparticles were prepared by dispersing 2 mg of polymer in 5 mL of ethanol: water mixture (1: 15 ratio), followed by sonication at 100 W. In case of spermine grafted PSMA, nanoparticles were formed by dispersing the polymeric derivative (2 mg) in DMSO (0.4 mL): 0.01 N HCl (4.6 mL) mixture. The obtained polymeric dispersion was sonicated, at 100 W, till appropriate particle size was achieved. Nanoparticulate dispersions were filtered using Amicon Ultra – 4 centrifugal filter device (Millipore) equipped with a 30 KDa membrane filter. The nanoparticles were then redispersed in milliQ water, lyophilized (labconco, 4.5 L) and stored at 4 °C. Average particle size and zeta potential of all nanoparticle formulations were measured using DLS (Malvern, zetasizer). The morphology of nanoparticles was studied using transmission electron microscopy (TEM).

Cytotoxicity studies

MTT assay was performed on MCF-7 and L929 cell lines, as per published protocol.[45 - 46] Cells were cultured on T-25 flasks in DMEM media, supplemented with 10% fetal bovine serum, at 37 °C and 5 % CO_2. Penicillin and streptomycin combination (1%) was used as antimicrobial agent. When the cells attained 80% confluency, they were trypsinized and seeded in to 96 well plate (10^4 cells/well). The cells were then incubated for 24 hours, at 37 °C and 5 % CO_2. Nanoparticles of various polymeric derivatives at different concentrations and polyplexes at various weight ratios of polymer/pDNA (5, 10, 15 and 20) were added to the wells, and incubated for 48 hours. Triton X 100 and phosphate buffer saline (pH 7.4) were used as positive and negative controls, respectively. After 48 hours of incubation, 10 µL of MTT solution (2.5 mg/mL) was added to each well, and further incubated for 4 hours. After removing the media, 100 µL of DMSO was added to each well, and readings were taken at 540 nm using microplate spectrophotometer (PowerWave XS2, Bio Tek Instruments, USA). The % cell viability was calculated according to following equation

$$\% \text{ Cell viability} = \left\{ \frac{\text{Absorbance of sample} - \text{Absorbance of Positive control}}{\text{Absorbance of negative control} - \text{Absorbance of Positive control}} \right\} \times 100$$

Haemolysis and endosomal rupturing capacity of nanoparticles

Haemolysis experiments were performed at two pH values viz.7.4 and 5.5, according to previously reported procedures.[47] Human red blood cells were isolated from whole human blood (collected from healthy human volunteers at IIT Delhi hospital, New Delhi), by centrifuging at 1500 rpm for 5 minutes. 30 µL of human red blood cells were diluted to 10 mL with phosphate buffer salines (pH 7.4 and 5.5), and rinsed three times with the corresponding buffer salines. The RBCs were then resuspended in corresponding buffers. 100 µL of polymeric dispersions in different buffer salines were mixed with 100 µL of RBC suspensions in the same buffer, at nanoparticle concentrations ranging from 50 – 1000 µg/mL. Then the mixtures were incubated at 37 °C for 30 minutes. After the incubation, dispersions were centrifuged at 1500 rpm for 10 minutes, and the supernatants were transferred to 96 well plate. The absorbance of supernatants was measured at 540 nm using micro plate spectrophotometer (PowerWave XS2, Bio Tek Instruments, USA). 1 % triton X 100 solution was used as positive control and respective buffer salines (pH 7.4 and 5.5) were used as negative controls. % haemolysis was calculated according to the following equation.

$$\% \text{ Haemolysis} = \left\{ \frac{\text{Absorbance of sample} - \text{Absorbance of negative control}}{\text{Absorbance of Positive control} - \text{Absorbance of negative control}} \right\} \times 100$$

Preparation and characterization of pDNA- polymer complexes

Nanoparticles of various polymeric derivatives were dispersed in DNase free water and mixed with equal volumes of red fluorescent protein (RFP) expressing pDNA (DsRed-Express-N1) solutions (in DNase free water), at various weight ratios (5, 10,15 and 20). The mixtures were vortexed for 30 seconds and incubated at room temperature for 30 minutes. DNA binding and condensation properties of polymeric nanoparticles were evaluated by performing agarose gel electrophoresis. The

complexes were mixed with gel loading buffer (5:1 ratio by volume), and loaded on 1% agarose gel containing ethidium bromide (0.5µg/mL of gel) in Tris –acetate-ethylenediamine tetra acetic acid. Electrophoresis was carried out for 120 minutes, at 70V. The bands of pDNA in the gel were observed using UV illuminator, and photographs were taken using molecular imager (Gel Doc XR, BIO RAD).

DNase I degradation assay of polyplexes

The efficiency of polymeric nanoparticles in protecting the complexed pDNA from enzymatic degradation was studied by treating the complexes with DNase I, according to standard procedures [48] with slight modification. The pDNA-nanoparticle complexes were incubated with DNaseI at a concentration of 1 U DNase/µg of pDNA, for 30 minutes, at 37 °C .Ethylenediamine tetra-acetic acid (EDTA) was then added to the enzyme-polyplex mixture, at a concentration of 2.5 mM, and the whole dispersion was heated for 10 minutes at 70 °C. The DNA molecules complexed to the polymeric nanoparticles were then released by treating with heparin at a concentration of 200 U/ µg of pDNA, for 30 minutes, at 37 °C. The released DNA molecules were analyzed using 1 % agarose gel electrophoresis.

In vitro transfection studies

Polyplexes of DsRed-Express-N1 were evaluated for their transfection efficiency on MCF-7 cells. Cells were seeded, at a density of 10^5 cells/well, into 24 well plates in the presence of 1 mL complete medium (DMEM). The seeded cells were incubated for 20 hours to obtain ~ 70 % confluency. The growth medium was then completely removed and replaced with fresh medium (without serum) containing polyplexes at different weight ratios. pDNA concentration used was 2 µg/well. After 4 hours of incubation, the medium was again replaced with complete growth medium and further incubated for 48 hours. The red fluorescent protein expressing cells were visualized using an inverted fluorescence microscope (Nikon Eclipse Ti, Japan) and the fluorescence measurements were performed using a fluorescence activated cell sorter (BD Accuri-C6, BD Biosciences). Untransfected cells were taken as negative control, and cells treated with polyplexes of branched PEI, 25,000 Da (at an optimal N/P ratio of 10) were employed as positive control. For the measurement of fluorescence, 10,000 events were counted.

Results and discussions

Synthesis and characterization of poly (styrene-alt-maleic anhydride) grafts

PSMA was characterized using ^{1}H NMR (Figure S.1, ESI†) and ATR-FTIR (Figure S.16, ESI†). ^{1}H NMR of PSMA is characterized by broad bimodal signals ranging from δ 1.8 - 3.6. These are attributed to methylene groups and tertiary carbons in the main chain of polymer. Styrene residues exhibit signals ranging from δ 7-7.6. Since low molecular weight PSMA is produced in cumene, using dicumyl peroxide as the initiator, polymeric chains are capped with terminal cumene residues. The proton signal at δ 1.25 was due to terminal methyl groups of cumene. ATR-FTIR of PSMA shows two characteristic absorption bands, due to the stretching vibrations of carbonyl groups of anhydride, at 1853 cm^{-1} and 1773 cm^{-1}. Different types of cationic structures were grafted to the polymer (PSMA) backbone to obtain their corresponding amphiphilic derivatives (Figure 1). To form quaternized polymeric grafts, derivatizing agents were selected from aromatic (isonicotinic acid), aliphatic (glycidyl trimethyl ammonium chloride) and cyclo aliphatic (1-(2-aminoethyl) piperazine) chemical families. L-arginine and spermine were employed as non quaternized derivatizing compounds. Rationale for synthesizing these different types of PSMA derivatives was to evaluate the impact of attached chemical structures in modulating the gene delivery efficacy of PSMA.

Synthesis of quaternized isonicotinic conjugated PSMA (P1)

Isonicotinic acid was grafted to PSMA using 3-amino-1-propanol. N-Boc protected 3-amino-1-propanol was synthesized (S.1, ESI†), and characterized using ^{1}H NMR (Figure. S.2, ESI†). It was then conjugated to isonicotinic acid through esterification (Scheme I), and the resultant product viz. 3-((tert-butoxy)-amino) propyl isonicotinate was characterized using ^{1}H NMR (Figure S.3, ESI†) and mass spectrometry (MALDI TOF/TOF^{TM}, USA) (Figure S.22, ESI†). ^{1}H NMR shows characteristic signals corresponding to methyl groups of Boc (δ 1.44) and aromatic protons (δ 7.8 and δ 8.7) . Further, the product formation was confirmed by mass spectra indicating peaks at 281 and 303, corresponding to $M+H^+$ and $M + Na^+$ respectively. The obtained conjugate was deprotected and grafted to PSMA backbone via amide linkages (Scheme I). ^{1}H NMR of PSMA grafted with isonicotinic acid shows symmetric signals at δ 7.8 and δ 8.9 (Figure S.4, ESI†), which confirms the presence of aromatic hydrogens of isonicotinic acid. For introducing cationic charge, the polymeric derivative was quaternized with methyl iodide (Scheme I).

^{1}H NMR spectrum of the quaternized isonicotinic acid derivative (Figure S.5, ESI†) depicts a strong signal at δ 3.9, which is assigned to the methyl groups attached to the nitrogen atoms of pyridine unit. ATR-FTIR of **P1** shows disappearance of bands (1853 cm^{-1} and 1773 cm^{-1}) due to carbonyl stretching of anhydride groups (Figure. S.17, ESI†), which indicates the hemi amide formation. – CH stretching frequency shows band around 2946 cm^{-1}. A slight shift in the value is due to the presence of strained side chain. A very strong band of the carbonyl group of ester appears at 1727cm^{-1}.The weak band at 1670 cm^{-1} confirms amide bond formation. The weak band indicates conjugation of the side chains. NH bending gives band at 1596 cm^{-1} in the spectrum, whereas CN stretching of the amide bond is indicated by absorption band at 1450 cm^{-1}.

Quaternized piperazine - PSMA conjugate (P2) formation and characterization

In the first step, 1-(2-aminoethyl) piperazine was conjugated to PSMA backbone via amide bond using dimethylformamide (DMF) as solvent. The product precipitated readily in the reaction medium and it has shown low solubility in various solvents tested, including water and DMSO. Intra- and/or inter- molecular hydrogen bonding, between the secondary nitrogens of attached piperazinyl groups and carbonyl groups of polymeric side chains, was the probable reason for this reduced solubility.[27] To impart cationic charge in the obtained polymeric graft, it was reacted

with methyl iodide in DMSO (Scheme II). The solubility of polymeric derivative was enhanced as the reaction progressed. After 24 hours, the product was completely soluble in DMSO, probably due to the elimination of hydrogen bonding. ^{1}H NMR of 1-(2-aminoethyl) piperazine grafted PSMA (Figure S.6, ESI†) in methanol–D4 (CD_3OD) containing one drop of trifluoroacetic acid (*d*) showed the presence of methylene goups of piperazine at δ 2.7 – 2.9. ^{1}H NMR of quaternized piperazine grafted PSMA in DMSO-*d*6 (Figure S.7, ESI†) exhibited signals due to methylene and methyl groups, in the vicinity of quaternary nitrogen atoms of the polymeric derivative **(P2)**, at δ 3.6 - 3.8. FT-IR spectrum of **P2** (Figure S.18, ESI†) displays strong band at 1713 cm^{-1}, indicative of stretching vibrations of carbonyl groups of carboxylic acid. Amide bonds in the polymeric derivative show bands at 1650 and 1560 cm^{-1}.

Synthesis of glycidyl trimethyl ammonium chloride grafted PSMA (P3)

Glycidyl trimethyl ammonium chloride was grafted to PSMA using 3-amino-1-propanol. N- Boc protected 3-amino-1- propanol (Scheme I) was grafted to PSMA through esterification (Scheme III), followed by deprotection of Boc. Both the polymeric derivatives were characterized using ^{1}H NMR and ATR-FTIR. ^{1}H NMR of N-Boc- 3-amino-1-propanol grafted PSMA (Figure S.8, ESI†) in DMSO-*d*6 shows a strong signal at δ 1.36, indicative of methyl groups of Boc whereas in the spectra of deprotected polymeric derivative (Figure S.9, ESI†), the signal due to Boc was completely disappeared. This confirms the formation of 3-amino-1-propanol grafted PSMA. In the second step, epoxy groups of glycidyl trimethyl ammonium chloride were conjugated to the free amino groups of 3-amino-1-propanol grafted PSMA under basic conditions (5 % NaOH). ^{1}H NMR of **P3** (Figure S.10, ESI†), in DMSO-D6, depicts a strong signal at δ 3.16 due to methyl groups of quaternary nitrogens. ATR-FTIR spectra of **P3** (Figure S. 19, ESI†) shows characteristic carbonyl stretching frequency of ester at 1725 cm^{-1}, and NH stretching at 3433 cm^{-1}, which confirms that grafting has occured.

Grafting of L-arginine to PSMA

L-arginine was also grafted to PSMA backbone using 3-amino-1-propanol. Primary amines of 3-amino-1-propanol grafted PSMA was conjugated to carboxylic acid groups of mesitylene- 2-sulfonyl and Boc protected arginine (Boc-Arg-Mts-OH) via DCC/NHS coupling. Boc-Arg-Mts-OH was chosen for the reaction in order to avoid intermolecular reaction between the aminoacid molecules, and because of easy cleavage and removal of mesitylene groups compared to other protecting groups like tosyl. ^{1}H NMR of Boc-Arg-Mts-OH grafted PSMA (Figure S.11, ESI†) shows sharp signals of methyl groups attached to mesitylene at δ 2.2 and δ 2.6, and tertiary butyl groups of Boc at δ 1.360. An additional sharp peak merged with the peaks of styrene residues of polymer, at δ 7.0 ppm, is due to aromatic protons of the mesitylene. The mesitylene-2-sulfonyl and Boc were removed by treating with a cleavage cocktail (Scheme IV), according to previously reported procedure[28]. L-arginine grafted PSMA (**P4**) formed a transparent gel, in DMSO-*d*6. This gel formation could be due to the hydrogen bonding between amines and carboxylic groups of polymer side chains. ^{1}H NMR spectra of **P4** (Figure S.12, ESI†) indicates absence of mesitylene and Boc signals, which confirms the product formation. ATR-FTIR spectra of **P4** (Figure S.20, ESI†) displays carbonyl stretching frequency at 1726 cm^{-1}, and amide bands at 1666 and 1450 cm^{-1}.

Conjugation of spermine to PSMA

Spermine grafted PSMA (**P5**) was prepared by reacting mono N-Boc-protected spermine with anhydride groups of the polymer. Spermine was selectively protected with Boc group for avoiding possible cross linking of PSMA chains. 1 equiv. of Boc anhydride was reacted with 4 equiv. of spermine, to yield mono N-Boc protected spermine (~ 90 % peak intensity) along with Bis Boc protected spermine (~ 25 % peak intensity) as indicated by mass spectra (Figure S.23, ESI†) . The crude extract was treated with 1 N HCl, to convert mono N-Boc protected spermine to salt form, and extracted with ethyl acetate to remove Bis Boc protected product. ^{1}H NMR of mono N-Boc protected spermine (Figure S.13, ESI†) in $CDCl_3$ shows characteristic signals of Boc at δ 1.44, and methylene groups at δ 1.53, δ 1.68, δ 2.66 and δ 3.18. Spermine grafted PSMA (**P5**) was obtained by conjugating mono-N-Boc protected spermine to anhydride molecules, followed by the cleavage of Boc.

^{1}H NMR of mono-N-Boc protected spermine (Figure S.14, ESI†) in CD_3OD shows a sharp signal at δ 1.36, indicative of methyl groups of Boc. When dispersed in DMSO, **P5** exhibited a turbid gel like consistency probably due to strong hydrogen bonding contributed by multiple amine functionalities in spermine. But the solubility was improved upon addition of water. ^{1}H NMR of **P5** (Figure S.15, ESI†) was recorded using CD_3OD : D_2O mixture, at 1:1 ratio, to which a drop of TFA (deuterated) was added. The absence of sharp signal at δ 1.36 indicated complete deprotection, and the presence of methylene groups of spermine in the polymeric graft was confirmed by peaks at δ 1.3, δ 1.7 and δ 3.1. ATR-FTIR of **P5** (Figure S.21, ESI†) displays characteristic frequency of carboxylic acid at 1726 cm^{-1}, and amide bands at 1669 cm^{-1} and 1543 cm^{-1}.

Formulation and characterization of polymeric nanoparticles

Due to their amphiphilic nature, all the PSMA derivatives self assembled in aqueous media to form stable nanoparticles. During the preparation of nanoparticles, formulation parameters viz. weight of the polymer, solvent: non solvent ratios and sonication amplitude were kept constant . The sonication time was increased for each formulation till no further decrease in particle size was observed, and chosen as the optimum sonication time. Zeta potential of various nanoparticle formulations were measured after dispersing in milliQ water and phosphate buffer saline (pH 7.4). Details of particle size, zeta potential and optimum sonication time for each polymeric derivative are given in table 1. Nanoparticles of quaternized derivatives viz. **P1**and **P3** were formulated using DMSO: water mixture as solvent: non solvent, respectively. They were completely soluble in the solvent phase viz. DMSO, and formed nanoparticles of optimized size range and lower polydispersity indices (PDI). Optimized nanoparticles of **P1** have shown a polydispersity index of 0.108 ± 0.01, and that of **P3** exhibited PDI of 0.122 ± 0.01. PDI of the nanoparticles of **P2** viz. 0.226 ± 0.035 indicates their comparatively heterogeneous particle size distribution w.r.t nanoparticles of **P1** and **P3**.

P4 and **P5** formed a gel like consistency, when dispersed in

DMSO. Formation of strong intra/inter molecular hydrogen bonding between the amines present in **P4** and **P5** might have contributed to this gel formation. On addition of aqueous phase and subsequent sonication, they formed stable nanoparticles with comparatively higer PDI than the quaternized ones. **P5** nanoparticles exhibited maximum PDI followed by **P4** nanoparticles (0.34 ± 0.04 and 0.292 ± 0.023 respectively). The replacement of hydrogen bonding between the solutes by the same between solvent and solute molecules, on addition of aqueous phase, was the probable mechanism for nanoparticle formation of **P4** and **P5**.

Table 1: Optimized parameters of nanoparticulate formulations

Polymeric derivative	Optimum sonication time (min)	Average particle size (nm)	Polydispersity index (PDI)	Zetapotential (mV) in water	Zeta potential (mV) in PBS (pH 7.4)
P1	0.5	94 ± 3.06	0.108 ± 0.01	42.61± 1.17	-15.02± 2.33
P2	1.5	112 ± 5.22	0.226 ± 0.035	46.15 ± 1.64	12.28±0.53
P3	1	107 ± 2.16	0.122 ± 0.01	30.18 ± 1.06	-17.18± 2.66
P4	2.5	134 ± 4.67	0.292 ± 0.023	32.01 ± 1.68	4.12± 0.71
P5	3	162 ± 6.82	0.34 ± 0.04	34.34 ± 3.4	12.16±1.39

Mean ± SD, $n = 3$

All the formulations exhibited positive zeta potential, when dispersed in milliQ water. But, they have shown reduced zeta potential in phosphate buffered saline (PBS,pH 7.4). In case of **P1**, zeta potential decreased from + 42.61 ± 1.17 to -15.02 ± 2.33, when dispersed in PBS pH 7.4. This decrease in zeta potential to negative side was due to the ionization of free carboxylic acid groups present in the polymer. These carboxylic anions could neutralize the positive charge contributed by quaternary nitrogens of isonicotinic acid, and hence contributed to reduction in zeta potential. **P2** also exhibited reduction in zeta potential from + 46.15 ± 1.64 to +12.28±0.53, with increase in pH. But zeta potential of **P2** nanoparticles didn't reduce to negative side, due to the presence of more quternanry nitrogens (contributed by piperazinyl side chains) in the polymeric side chains. The reduction in zetapotential of **P3** nanoparticles from + 30.18 ± 1.06 to -17.18± 2.66, when dispersed in PBS, pH 7.4, could also be envisaged to the above mentioned reason.

L-arginine grafted PSMA nanoparticles have retained some positive charge viz. +4.12± 0.71. This could be due to the property of the guanidino groups of L-arginine to remain protonated and positively charged, at physiological pH.[29-30] Spermine grafted PSMA nanoparticles have also shown a reduction in zeta potential from + 34.34 ± 3.4 to +12.16±1.39. Spermine is a multivalent organic cation.[31] At physiological pH, the amines present in spermine get protonated.[32] Due to the protonation of primary and secondary amines, spermine grafted PSMA nanoparticles retained positive zeta potential in PBS, pH 7.4.

High resolution transmission electron microscopy (HR-TEM) images of the nanoparticles (Figure 2) showed core shell morphology, attributed to the amphiphilic nature of polymeric derivatives.[33] The particle size of nanoparticles obtained in HR-TEM were lesser than that of the DLS measurements. This could be explained on the basis of the formation of a hydrodynamic layer around the nanoparticles, when they were dispersed in water. DLS measures this hydrodynamic diameter, which in turn contribute to increased particle size.[34] The difference in particle size between DLS and HR-TEM measurements were more pronounced in case of quaternized derivatives, probably due to their minimal intermolecular hydrogen bonding and the resultant enhanced solubility in solvent phase. **P1** exhibited a particle size range of ~ 30- 65 nm in HR-TEM, whereas the DLS measurements of the same resulted in an average paricle size (Z average) of 94 ± 3.06 nm. HR-TEM image of **P2** nanoparticles also shown narrow particle size range of ~ 40 -70 nm in comparison to the average DLS particle size of 112 ± 5.22 nm. Average particle size of **P3** nanoparticles measured by DLS was 107 ± 2.16, in comparison to the lower particle size range of 42-56 nm obtained in HR-TEM.

HR-TEM images of the nanostructures formed by **P4** and **P5** showed that the particles were of 30-70 nm and 60-120 nm size range, respectively. The wide range of particle size distributions observed in **P4 and P5** indicates their comparatively high polydispersed nature. *In vitro* stability of the nanoparticles was examined by dispersing them in normal saline, and measuring the particle size and PDI at different intervals, up to 24 hours (data not shown). No significant change in the particle size or PDI was observed for any of the formulations tested.

The core shell type morphology of nanoparticles depicts their ability for incorporating both drugs and genes. Combinatorial delivery of anticancer drugs and gene therapy agents, viz. siRNA, shRNA, miRNA etc. are gaining importance in the cancer therapy.[35,36,37] Another advantageous feature of these low molecular weight PSMA nanoparticles is their *in vivo* biodegradability. Since the derivatizing agents of PSMA are linked via ester or amide bonds to the polymer backbone they can be easily cleaved through enzymatic hydrolysis, within the biological system, facilitating their elimination from the body. After the hydrolytic cleavage of ester or amide bonds *in vivo,* the low molecular weight PSMA derivatives will get converted in to small units with reduced molecular weight and enhanced solubility.[38] These small polymeric fragments can be easily degraded and eliminated .[39] This is a major advantage of low molecular weight PSMA over high molecular weight ones, the

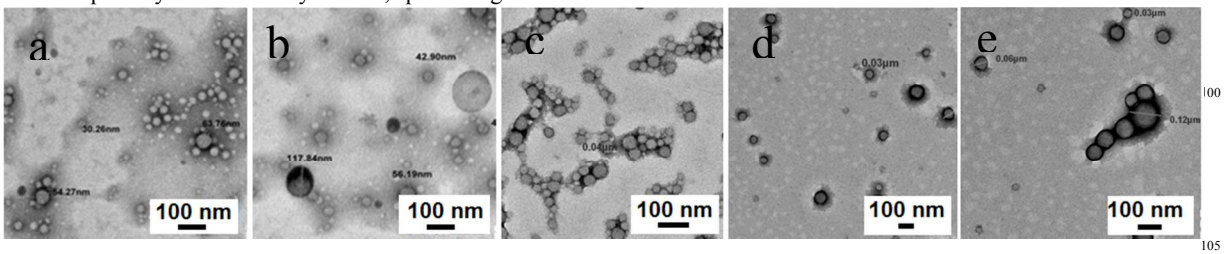

Figure 2. HR-TEM images of the nanoparticles of (a) **P1** (b) **P2** (c) **P3** (d) and **P4** (e) **P5**. All samples were prepared by drop-casting the aqueous dispersion of the respective polymer samples on copper grid and positively stained by phosphotungstic acid.

biodegradability of later being an obstacle for *in vivo* application. In addition, due to the amphiphilic and self assembling properties of these polymeric grafts, large scale production of their nanoparticles is feasible.[40] Formulation of stable nanoparticles of various PSMA derivatives were easily accomplished, without the use of excipients like surfactants, co-surfactants etc. This cost effective production and high stability makes them an attractive vehicle for intracellular delivery. Hence, developing pharmaceutical formulations based on these polymers are not challenging.

Cytotoxicity studies

Cytotoxicity of all the nanoparticle formulations was evaluated in two cell lines viz. MCF-7 and L929. Concentrations of nanoparticles tested were in the range of 50- 1000 µg/mL. The cells were treated with various nanoparticle formulations for 48 hours, and the % cell viability was assessed by MTT assay (figure 3). At 1000 µg/mL, **P1** has shown 72 % and 56 % cell viability, respectively in MCF-7 and L929 cell lines. The viability of cells seemed to be increased with lowering the nanoparticle concentrations. The % cell viability of **P1** nanoparticles were increased to 99 % and 88 %, respectively in MCF-7 and L929 cell lines, at the lowest concentration tested viz. 50 µg/mL. **P3** has also shown a similar pattern of increase in cell viability, at lower concentrations of nanoparticles tested. At 50 µg/mL concentration, **P3** nanoparticles achieved more than 94 % cell viability in L929 cells, and showed no toxicity in MCF -7 cells. Cytotoxic effects of **P2** nanoparticles were significantly higher than that of **P1** and **P3**. Maximum cell viability observed for **P2** nanoparticles were 69 % and 77 %, respectively in MCF-7 and L929 cells, at 50 µg/mL. This pronounced cytotoxic effect could be due to the presence of quaternized piperazine side chains with more cationic charge densities and their interaction with the cell membranes. Lower cationic charge densities and extensive shielding by surface carboxylic acid side chains of polymer backbone could be the reasons for comparatively lower cytotoxicities of **P1** and **P3**.[41] For finding out safer concentration range of **P2** nanoparticles, we have performed cytotoxicity studies at concentrations below 50 µg/mL. **P2** nanoparticles exhibited more than 90 % viability at 20 µg/mL, in both the cell lines (data not shown).

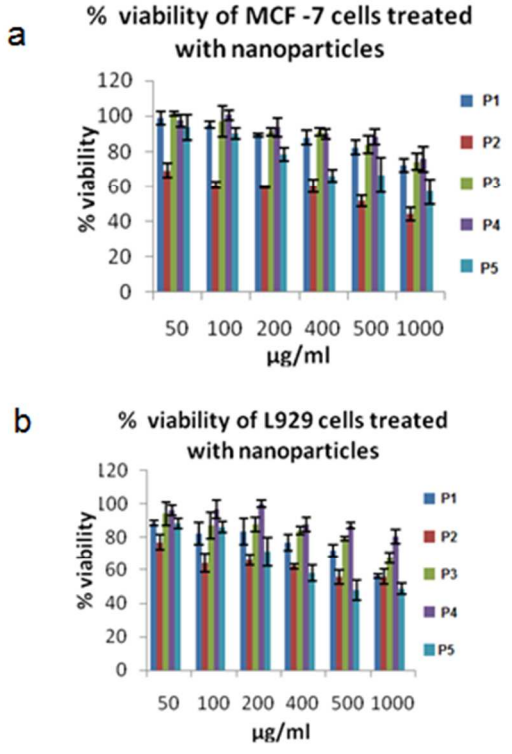

Figure 3. % cell viability of various nanoparticles in (a) MCF -7 cell lines and (b) L929 cells; (Mean ± SD, n = 3). Concentrations of nanoparticles (µg/mL) are represented in x-axis.

L-arginine grafted PSMA (**P4**) nanoparticles also exhibited minimal cytotoxicity at various concentrations tested. They have shown cell viability values of 75 % and 80% in MCF-7 and L929 cells, respectively, at the maximum concentration tested (1000 µg/mL). Below 200 µg/mL, no cytotoxicity was observed for **P4**. Spermine grafted PSMA (**P5**) nanoparticles exhibited significant cytotoxicity at higher concentrations, in both cell lines. Cell viability of **P5** nanoparticles at 1000 µg/mL were 56 % and 48 %, respectively in MCF-7 and L929 cells. Below 100 µg/mL, **P5** nanoparticles have shown more than 85 % cell viability in both the cell lines. L-arginine moieties in **P4** have very basic side chains and their guanidine groups are positively charged at physiological pH. But the shielding by negatively charged carboxylic acid groups of polymer backbone could have minimized the interaction of gaunidinium groups with the cell membrane. This was the probable reason for the minimal cytotoxicity of **P4** nanoparticles at various concentration tested. In case of **P5**, multiple protonating sites in the grafted spermine molecules induced more cationic charge, and thereby cytotoxicity. But the cytotoxic behaviour of spermine grafted PSMA nanoparticles were dose dependent, and they were safer to cells at concentrations (100 µg/mL and below) suitable for *in vivo* gene delivery applications.

Blood compatability and endosomal release properties of nanoparticles

For evaluating blood compatability and endosomal release properties, haemolysis of nanoparticles was studied at two different pH values, viz. 7.4 and 5.5. Haemolytic behaviour of nanoparticles at pH 7.4 indicates their blood compatibility, whereas the same at 5.5 could provide information regarding their ability to overcome endosomal uptake. Membrane destabilizing polymers can cause haemolysis at the similar pH values of endosomes (5.5-5.8).[12] Hence, the haemolytic behaviour of these particles at pH 5.5 can be correlated with their endosomal release. The % haemolysis of various nanoparticle formulations are shown in figure 4. The results indicated that, the haemolytic effects of all the formulations tested were directly proportional to the concentrations of nanoparticles.

Nanoparticles of quaternized polymeric derivatives viz.**P1**, **P2** and **P3** have shown almost similar pattern of haemolysis, at pH 7.4. Maximum % haemolysis shown by **P1**, **P2** and **P3** were, 4.83± 0.85, 6.13 ± 0.4 and 4.08 ± 1.33 respectively, at 1000 µg/mL. This significantly low haemolysis at physiological pH shows their excellent blood compatibility. Ionization of carboxylic acid groups of these quaternized polymeric derivatives at physiological pH and the resultant reduction in their surface positive charge (Table 1) might have contributed to the minimal

haemolysis. At pH 5.5, **P1** has shown significantly higher % haemolysis compared to **P2** and **P3** (Figure 4 B). Maximum % haemolysis of 86.51 ± 3.2 and minimum % haemolysis of 17.17 ± 1.35 was obtained for **P1**, at the respective nanoparticle concentrations of 1000 µg/mL and 50 µg/mL. This high % haemolysis observed for **P1**, at pH 5.5, could be due to the membrane destabilizing effect of quaternized aromatic side chains of the polymer. Hydrophobic aromatic chains imparted with positive charge can get easily incorporated in to the RBC membrane and cause their destabilization. The role of hydrophobic polymeric side chains in enhancing haemolysis at acidic pH has been experimentally reported by Henry et al.[12]

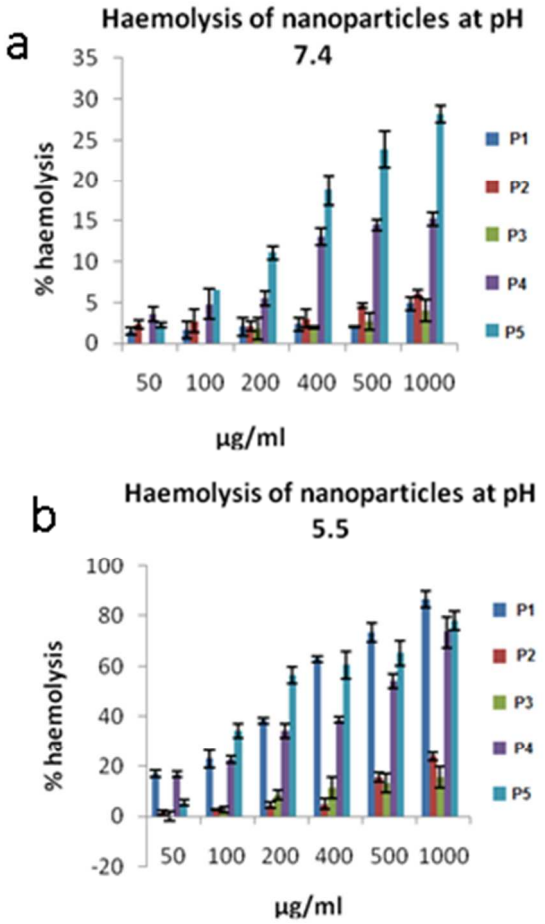

Figure 4. Haemolytic assay of various nanoparticulate formulations at (a) pH 7.4 and (b) pH 5.5 (Mean ± SD, *n* = 3). Concentrations of nanoparticles (µg/mL) are represented in x-axis.

P2 and **P3** exhibited a moderate increase in % haemolysis at pH 5.5 (24.04 ± 1.64 and 15.68 ± 4.07 respectively, at 1000 µg/mL), compared to that at pH 7.4. Eventhough **P1**, **P2** and **P3** possess same features viz. unionized and protonated state of the carboxylic groups of polymeric side chains and the presence of quaternary nitrogens providing cationic charge, % haemolysis of **P1** at 1000 µg/mL was 3.6 fold higher than **P2** and 5.5 fold higher than **P3**. This variation in haemoreactivity could be explained by the fact that, quaternized aromatic side chains of **P1** were able to disturb the inner parts of RBC membrane structure more effectively [42] than the quaternized aliphatic groups of **P2** and **P3**. From these results, it is clear that the presence of quaternary nitrogens in the polymeric side chains alone cannot induce haemolysis, because of their inability to bind protons and promote osmotic lysis of RBC membrane. Presence of hydrophobic groups in the polymer side chains play a crucial role in RBC lysis at acidic pH (5.5), and hence the same can promote membrane rupture at endosomal pH conditions.

L-arginine grafted PSMA and spermine grafted PSMA nanoparticles have shown considerable haemolysis at pH 7.4. At 1000 µg/mL, **P4** showed 15.27 ± 0.79 % and **P5** induced 28.2 ± 1.08 % haemolysis. But with decrease in concentrations of the nanoparticles of **P4** and **P5**, their haemoreactivity also reduced. **P4** and **P5** have shown a minimal % haemolysis of 3.61 ± 1.86 % and 2.28 ± 0.34 % respectively, at 50 µg/mL concentration. For gene delivery applications, 50 µg/mL is a significantly higher concentration. In addition, we have performed haemolytic experiments in saline buffer with washed RBC's inspite of serum or whole blood. Reports are suggesting that, plasma proteins present in the blood can bind polycations and thus reduce their affinity towards RBC's.[43] ie. in actual physiological conditions of blood (pH 7.4), the haemolytic effect of these polymeric nanoparticles could be further lowered.

Both **P4** and **P5** have shown higher haemolysis at pH 5.5, due to the presence of primary and secondary nitrogens in their side chains which can bind protons at acidic pH and promote membrane lysis. Nanoparticles of **P4** and **P5** incubated with RBC's at pH 5.5 have shown maximum % haemolysis of 73.52 ± 6.2 and 78.05 ± 3.89, respectively, at 1000 µg/mL. They have also shown higher % haemolysis at all concentrations in pH 5.5, compared to corresponding concentrations in pH 7.4. This could be due to the binding of protons to the primary and secondary amines in acidic pH. The protonation of primary and secondary amines will be accompanied by counter flow of anions and subsequent increase in osmotic pressure, which is responsible for the rupturing of RBC membrane. Similar mechanism is also responsible for the endosomal membrane rupture and is termed as proton sponge effect.[44] From the haemolytic study of different polymeric derivatives, we have concluded that the major driving forces for promoting membrane rupture at endosomal pH are (i) membrane destabilization by the hydrophobic side chains and (ii) proton sponge effect produced by the protonation of primary or secondary amines present in the polymeric systems.

Formulation of polyplexes and their evaluation

Polyplex formation was achieved via electrostatic interactions between the phosphate groups of DNA base pairs and amine groups of polymeric nanoparticles. In addition, aromatic groups and amide linkages present in the polymeric derivatives can interact via hydrogen bonding to the DNA base pairs .[13] Gel retardation of pDNA in the polyplexes gives clear cut information regarding the DNA binding and condensation efficiency of the cationic polymeric nanoparticles. For the gel retardation study, we have kept the amount of pDNA constant at 1 µg, and varied the amount of polymeric nanoparticles. For comparative evaluation of different polyplexes, polymer/pDNA weight ratios of 20, 15, 10 and 5 were chosen. The selection of these weight ratios were based on the cytotoxic profile of polymeric nanoparticles .The maximum polymer/pDNA weight ratio selected was 20, equivalent to a concentration of 100 µg/mL of polyplex when dispersed in 96 wells containing 200 µL of media.

Similarly, lower weight ratios viz. 5, 10 and 15 corresponded to polyplex concentrations of 25, 50 and 75 µg/mL, respectively. Since nanoparticles of all the polymeric derivatives have shown reduced zeta potentials at physiological pH , their complex formation with pDNA was carried out in DNase free water (neutral pH). This was to prevent ionization of carboxylic acid groups in the polymer side chains, and there by facilitating retardation properties of **P1** and **P2**, when compared to **P3**. L-arginine conjugated PSMA (**P4**) and spermine grafted PSMA (**P5**) have shown efficient gel retardation of pDNA, at all weight ratios tested. This could be attributed to the ability of guanidino groups of L-arginine and multivalent cations of spermine to get protonated and retain positive charge, at physiological pH. The pattern of pDNA binding in the polyplexes of **P4** and **P5** seemed

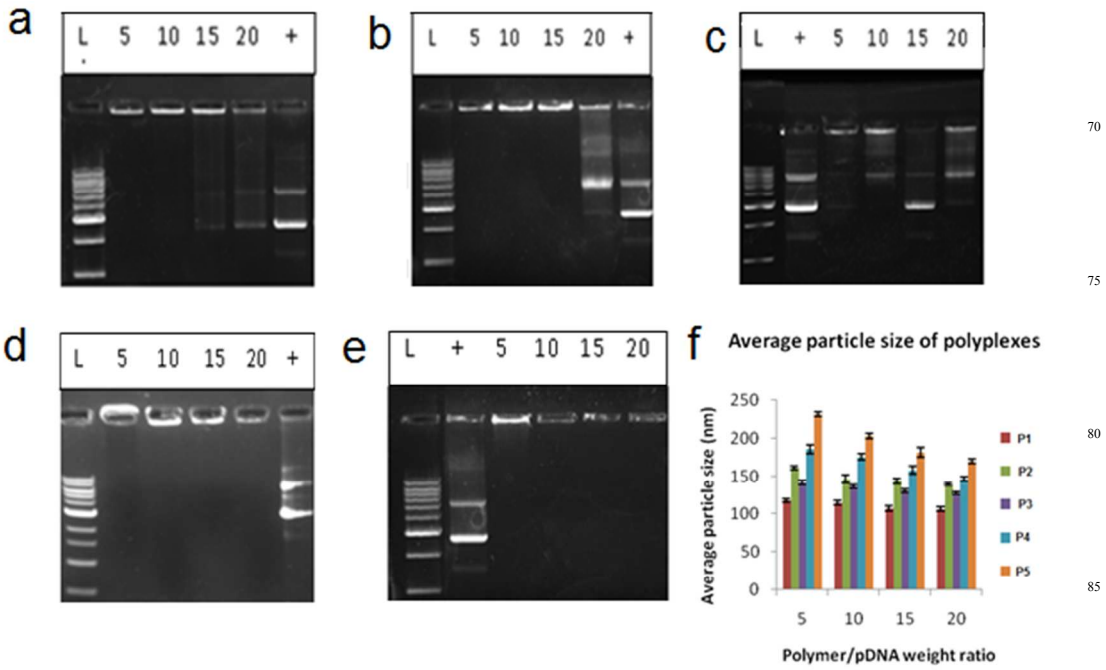

Figure 5. Agarose gel (1 %) electrophoresis showing bands of complexed pDNA in polyplexes of (a) **P1** (b) **P2** (c) **P3** (d) **P4** and (e) **P5**. 5, 10, 15 and 20 are the weight ratios of the polymer to pDNA. L represents ladder and + is pure pDNA (control) (f) Average particle sizes of polyplexes at different polymer/DNA weight ratios (Mean ± SD, n = 3).

efficient complex formation. Gel retardation of the pDNA by various PSMA derivatives, at different weight ratios, is shown in figure 5.

Polyplexes of **P1** have shown maximum retardation at lower polymer to pDNA weight ratios (5 and 10), and comparatively increased DNA release at higher ratios viz.15 and 20. Quaternized piperazine grafted PSMA (**P2**) exhibited efficient gel retardation at weight ratios viz. 5, 10 and 15, whereas proper binding and condensation of pDNA was not observed at polymer/pDNA weight ratio of 20. The carboxylic acid groups of polymer side chains can ionize in gel loading buffers (pH 7.4) and induce electrostatic repulsive forces. This could be the reason for reduced gel retardation of pDNA at higher weight ratios. The electrostatic repulsive effect was more pronounced in case of **P3**, as shown in figure 5, where minimal retardation was observed at all weight ratios tested. Polyplexes of **P3** incorporated the pDNA predominantly through the cationic charges of glycidyl trimethyl ammonium chloride side chains. But in case of **P1**, additional binding forces viz. π-π stacking of aromatic side chains (isonicotinic acid) and hydrogen bonding of amide linkages could also take part in polyplex formation. **P2** possesses more cationic charge densities due to the presence of two quaternary nitrogens per monomer unit, and remains positively charged at physiological pH. These could be the reasons for better gel to be in reverse manner to that of the quaternerized ones. As polymer/pDNA weight ratios were increased, more efficient binding and condensation of DNA were observed in **P4** and **P5**. This shows that, the primary and secondary amines present in **P4** and **P5** could effectively neutralize the electrostatic repulsive forces produced by the ionization of carboxylic acid groups.

Cell viability studies of polyplexes in MCF-7 and L929 cells indicated that, polyplexes of all the polymeric derivatives, except **P2**, were safer at different weight ratios tested (data not shown). But polyplexes of **P2** have shown increased % cell viability compared to the corresponding concentrations of uncomplexed nanoparticles. This could be due to the neutralization of surface cationic charge by complexed pDNA molecules. Further, at polymer/ DNA weight ratio viz. 5, polyplexes of **P2** exhibited more than 90 % cell viability in both the cell lines. The polyplexes were also evaluated for their particle size and zeta potential, using DLS, by dispersing them in milliQ water. Particle size of various polyplexes exhibited slight to moderate increase with decrease in the polymer/pDNA weight ratio (Figure 5.f).

At higher weight ratios of polymer/pDNA, more cationic binding sites are available, which leads to better condensation of complexed pDNA. Hence, average particle sizes of polyplexes increased with lowering the weight ratios. We have observed that, less polydispersed nanoparticles viz. **P1** and **P3** have shown

slight increase in particle size with decrease in weight ratio, whereas moderate increase in particle size was obtained for polyplexes of **P2**, **P4** and **P5**, whose PDI values were comparatively higher. Maximum particle sizes were obtained for the polyplexes of **P5**, whose average size increased from 169.6 ± 3.1 to 231.8 ± 2.1, with respective decrease in polymer/DNA weight ratios from 20 to 5. Zeta potentials of all polyplexes have shown slight decrease with the decrease in polymer/DNA weight ratio, due to the consequent reduction in cationic surface charge (data not shown). Maximum zeta potential was obtained for polyplexes of **P2** (+ 47.5 ± 2.54), at the polymer/DNA weight ratio of 20. The zeta potential was reduced slightly to + 43.62 ± 3.8, with the corresponding decrease in weight ratio to 5. Other polyplexes also exhibited similar pattern of variation in zeta potential, w.r.t polymer/DNA weight ratio.

DNase I protection assay.

The efficiency of various polyplexes to protect complexed DNA was evaluated by treating with DNase I. Stable electrostatic interactions are required for efficient binding and condensation of DNA in the nanoplexes. The results of DNase I degradation study of various polyplexes are shown in figure 6. Spermine grafted PSMA nanoplexes have shown efficient condensation and protection of pDNA, at all weight ratios tested (Figure 6A). At higher weight ratios viz. 20 and 15, the binding and condensation were strong enough to prevent the release of DNA, even after treatment with heparin. This could be due to the strong electrostatic interaction of the multivalent cations of spermine towards pDNA. At lower weight ratios of **P5** viz. 5 and 10, pDNA showed release from the polyplexes.

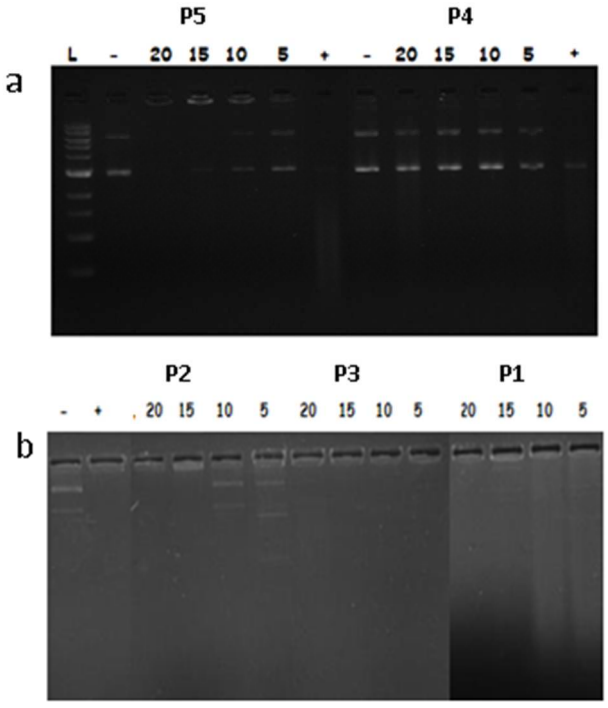

Figure 6. DNA release from the polyplexes of (a) **P4** and **P5** (b) **P2**, **P3** and **P1** at different weight ratios (20, 15, 10 and 5) after treatment with DNase and heparin. L represents ladder, - indicates untreated pDNA and + shows treated pDNA.

L-arginine grafted PSMA nanoparticles were also effective in protecting pDNA from DNase degradation, as indicated by the release of DNA from their polyplexes. The ability of guanidino groups of L-arginine for binding and condensing pDNA, due to their cationic nature at physiological pH, is well established.

In case of quaternized polymeric grafts (**P1**, **P2** and **P3**), the surface cationic charge of nanoparticles had significant role in the protection of pDNA against DNase I (Figure 6B). Polyplexes of **P1** exhibited complete degradation of DNA at higher weight ratio viz. 20. At lower weight ratios of **P1**, DNA bands were observed, but the conformation of released DNA seemed to be changed. This could be due to the partial digestion by DNase I. In case of **P2**, weight ratios of 5 and 10 have shown efficient protection of Polyplexes of **P3** exhibited complete digestion of pDNA, at all weight ratios tested. The positive surface charge of the nanoparticles of **P2**, in physiological pH (table 1), might have contributed to their stable binding and condensation of DNA. Nanoparticles of **P1** and **P3** were not able to condense DNA efficiently, due to their surface negative charge in physiological pH and electrostatic repulsive forces of carboxylic acid groups of PSMA. Hence they could not afford protection against DNase I. This indicates that, **P1** and **P3** need further chemical modification to enhance their efficiency for condensing and protecting DNA in physiological conditions.

In vitro transfection efficiency

L-arginine and spermine grafted polyplexes were selected for in vitro transfection studies based on their efficient complex formation, resistance to DNase and endosomal rupturing properties. Transfection efficiency of these polyplexes, at different weight ratios, was evaluated using MCF-7 cells as a model cell line. Polyplexes were suitably formulated and incubated with the cells in serum free media, up to 4 hours. This was to avoid the interference of proteins present in serum with the cellular uptake of polyplexes.

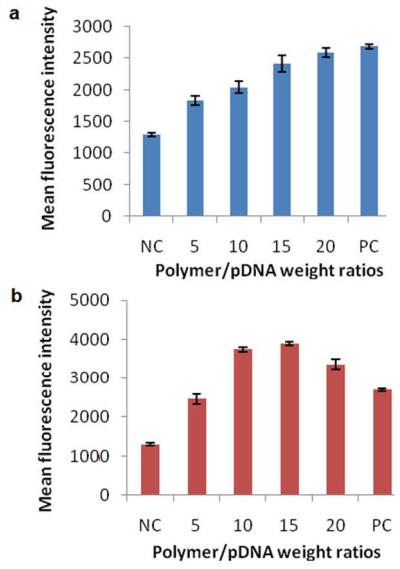

Figure 7. Transfection efficiency of the polyplexes of (a) **P4** and (b) **P5** at different weight ratios viz. 5,10,15 and 20 in MCF-7 cell line (Mean ± SD, *n* = 3). NC – untransfected cells (negative control); PC – PEI, 25000 Da – DNA complex at optimal N/P ratio of 10 (positive control).

permine grafted polyplexes exhibited comparable transfection efficiencies to that of PEI 25,000 Da, at weight ratios of 5 and 10, and even better efficiency (1.45 fold higher) at weight ratio of 15. Transfection efficiency of spermine grafted polyplexes was slightly reduced at weight ratio of 20, indicating a possible triggering of cytotoxic effect. In case of L-arginine grafted polyplexes, tansfection efficiency enhanced with the increase in weight ratio and reached almost comparable to positive control, at weight ratios of 15 and 20. The fluorescence quantification of cells treated with various polyplexes and images of the same (at 10 x magnification) are represented in figures 7 and 8, respectively. The transfection studies indicate that polyplexes of L-arginine and spermine can be employed at significantly higher concentrations, without cytotoxic effects, for gene delivery applications. Most of the conventional transfection agents shows cytotoxicity at concentrations suitable for *in vivo* applications. Hence developing a safe formulation for *in vivo* gene delivery is challenging. In this context, PSMA derivatives viz. **P4** and **P5** show potential for therapeutic applications.

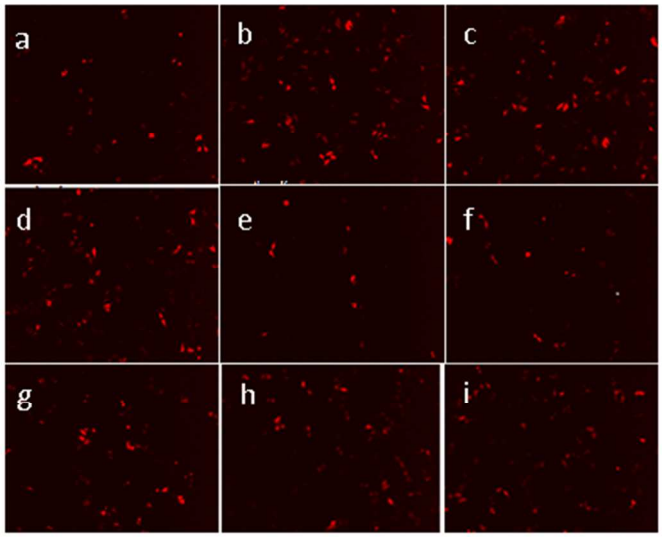

Figure 8. Fluorescence images of MCF-7 cells transfected with polyplexes of **P5** in polymer/pDNA weight ratios (a) 5 (b) 10 (c)15 (d) 20, **P4** in polymer/pDNA weight ratios (e) 5 (f) 10 (g) 15 (h) 20 and (i) PEI (25,000 Da) at optimal N/P ratio = 10.

Among the various quaternized compounds evaluated, quaternized isonicotinic acid need special attention. Maximum endosomal rupturing property (% haemolysis at pH 5.5) was achieved by the hydrophobic isonicotinc acid units, compared to the other derivatizing agents. This indicates that PSMA embedded with hydrophobic cations can escape endolysosomes to achieve efficient transfection. Cytotoxic potential was also low for **P1**. The only drawback of **P1** as an efficient gene delivery agent was its susceptibility to probable electrostatic repulsive forces from their carboxylic acid counter parts. To overcome this, free carboxylic functional groups of PSMA side chains can be derivatized with various biocompatible moieties. This would minimize the electrostatic repulsive forces of carboxylate ions and enhance the DNA condensation efficiency of embedded cations. Thus, grafting of PSMA with hydrophobic cations could be employed as an excellent strategy for gene delivery applications. **P2** and **P3** didn't exhibit significant haemolysis at pH 5.5, indicating their limited potential for endolysosomal uptake. Hence we can hypothesize that, grafting of hydrophilic quaternary compounds to PSMA will not be an effective method for achieving intracellular gene delivery. PSMA derivatized with primary/secondary amine containing compounds (**P4**, **P5**) depicted all round excellence as gene delivery vehicles. An overall summary of our research outputs is represented graphically in figure 9.

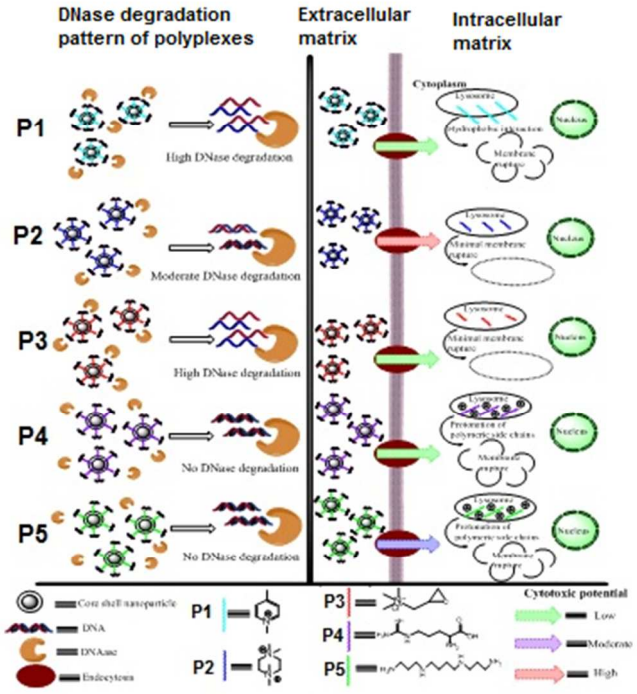

Figure 9. Graphical represention of intracellular gene delivery properties of various PSMA derivatives **P1**-**P5**.

Conclusions

Intracellular gene delivery application of low molecular weight PSMA was explored by grafting different types of cationic groups to the polymer backbone. All the polymeric derivatives readily formed core shell type nanoparticles. Grafting of L-arginine and spermine to PSMA backbone depicted endosomal escape properties, strong binding and condensation of pDNA molecules, efficient protection against DNase I and excellent transfection. The quaternized polymeric derivatives have shown their own advantages and disadvantages as intracellular delivery vehicles w.r.t their chemical composition. **P1** exhibited strong endosomal rupturing property, due to the presence of hydrophobic aromatic side chains, and were able to bind pDNA effectively at lower polymer/DNA weight ratios tested. But due to the electrostatic repulsion of carboxylic groups, at physiological pH, they were not effective in protecting DNA against DNase I degradation. Polyplexes of **P2** were able to overcome DNase degradation at lower weight ratios. However, dose dependent cytotxicity was their disadvantage. **P3** nanoparticles were not effective in complexing pDNA. Through suitable chemical modifications, to overcome the lacunae viz. cytotoxicity, inefficient protection against DNsae degradation

etc., the quaternized derivatives may also be developed in to efficient gene delivery formulations. Simplicity of nanoparticle preparation, feasibility of combinatorial delivery of genes and drugs due to the core shell structure, enhanced biodegradability due to low molecular weight etc. strongly suggest that, the nanoparticles of PSMA derivatives can be employed as efficient intracellular delivery vehicles for therapeutic applications.

Acknowledgements

Aji Alex M.R is thankful to Electron Microscopy Facility, All India Institute of Medical Sciences (AIIMS), New Delhi, India for TEM studies and Indian institute of Technology, Delhi for awarding Institute Fellowship. He is also grateful to Mr. Asif.S, PhD scholar, National Institute of Immunology (NII), New Delhi, India for help with the flow cytometry studies.

Notes and references

[a] *Centre for Biomedical Engineering, Indian Institute of Technology Delhi, New Delhi 110016, India*
Tel: + 91 1126591041
Email: veenak_iitd@yahoo.com
[b] *Biomedical Engineering Unit, All India Institute of Medical Sciences, New Delhi 110029, India*
[c] *Department of Biochemical Engineering and Biotechnology, Indian Institute of Technology Delhi, New Delhi 110016, India*

† Electronic Supplementary Information (ESI) available: [Synthetic procedures, NMR, ATR-FTIR and MALDI spectra]. See DOI: 10.1039/b000000x/

‡ Footnotes should appear here. These might include comments relevant to but not central to the matter under discussion, limited experimental and spectral data, and crystallographic data.

1. X. Guo, L. Huang, Acc. Chem.Res. 2012, 45, 971-979.
2. D.Putnam, Nat.Mater. 2006, 5, 439-451.
3. A. Sopahun, S. Abliz, I. Nurulla, Guang pu xue yu guang pu fen xi Guang pu 2012, 32, 1677-1680.
4. J.Han, P. Silcock, A.J.McQuillan, P. Bremer, Colloid Polym Sci. 2008, 286, 1605-1612.
5. C.A.Lackey, O.W. Press, A.S. Hoffman, P.S. Stayton, Bioconjugate Chem. 2002, 13, 996-1001.
6. H. Maeda, M. Ueda, T. Morinaga, T. Matsumoto, J. Med. Chem. 1985, 28, 455-461.
7. T. Konno, Eur. J. Cancer 1992, 28, 403-409.
8. K.Greish, T. Sawa, J. Fang, T. Akaike, H. Maeda, J. Controlled Rel. 2004, 97, 219-230.
9. K. Greish, A. Nagamitsu, J. Fang, H. Maeda, Bioconjugate Chem. 2004, 16, 230-236.
10. Y.Mu, H. Kamada,Y. Kaneda, Y. Yamamoto, H. Kodaira,S.Tsunoda, Y. Tsutsumi, M. Maeda, K.Kawasaki, M. Nomizu,Y. Yamada, T. Mayumi, Biochem. Biophys. Res. Commun. 1999, 255, 75-79.
11. H. Maeda, Adv. Drug Deliv. Rev. 2001, 46, 169-185.
12. S.M.Henry, M.E.H.El-Sayed, C.M. Pirie, A.S. Hoffman, P.S. Stayton, Biomacromolecules 2006, 7, 2407-2414.
13. X.Duan, J.Xiao, Q. Yin, Z. Zhang, S. Mao, Y. Li, Int.J.Nanomed. 2012, 7, 4961-4972.
14. V. Judge, B. Narasimhan, M. Ahuja, D. Sriram, P. Yogeeswari, E. De Clercq, C. Pannecouque, J. Balzarini, Med Chem Res. 2012, 21, 1451-1470.
15. I. Chevrier, J.L. Sague, P.S. Brunetto, N. Khanna, Z. Rajacic, K.M. Fromm, Dalton Trans. 2013, 42, 217-231.
16. J.J. Thomas, M.R. Rekha, C.P. Sharma, Int. J.Pharm. 2010, 389, 195-206.
17. Y. Ping, D. Wu, J.N. Kumar, W. Cheng, C.L. Lay, Y. Liu, Biomacromolecules 2013, 14, 2083-2094.
18. R.Q. Li, Y.L. Niu, N.N. Zhao, B.R. Yu, C. Mao, F.J. Xu, ACS Appl. Mater. Interfaces 2014, 6, 3969-3978.
19. S. Patnaik, R. Goyal, S.K. Tripathi, M. Arif, K.C. Gupta, RSC Adv. 2012, 2, 4335-4342.
20. T.I. Kim, M. Ou, M. Lee, S.W. Kim, Biomaterials 2009, 30, 658-664.
21. K. Nam, H.Y. Nam, P.H. Kim, S.W. Kim, Biomaterials 2012, 33, 8122-8130.
22. Y. Lee, H.Y. Nam, J. Kim, M. Lee, J.W. Yockman, S.K. Shin, S.W. Kim, Mol Ther 2012, 20, 1360-1366.
23. R. Amini, F.A. Jalilian, S. Abdullah, A. Veerakumarasivam, H. Hosseinkhani, A.S. Abdulamir, A.J.Domb, D. Ickowicz, R. Rosli, Appl Biochem Biotechnol 2013, 170, 841-853.
24. J.R. Viola, H. Leijonmarck, O.E. Simonson, I.I. Oprea, R. Frithiof, P. Purhonen, P.M.D. Moreno, K.E.Lundin, R. Stromberg, C.I.E. Smith, Gene therapy 2009, 16, 1429-1440.
25. M.A. Maslov, T.O. Kabilova, I.A. Petukhov, N.G. Morozova, G.A. Serebrennikova, V.V.Vlassov, M.A. Zenkova, J. Controlled Rel. 2012, 160, 182-193.
26. S.A.Chew, M.C. Hacker, A. Saraf, R.M. Raphael, F.K. Kasper, A.G.Mikos, Biomacromolecules 2010, 11, 600-609.
27. P.J.M. Stals, M.A.J. Gillissen, R. Nicolay, A.R.A. Palmans, E.W. Meijer, Polym. Chem. 2013, 4, 2584-2597.
28. A.Isidro-Llobet, M. Álvarez, F. Albericio, Chem. Rev. 2009, 109, 2455-2504.
29. M. Kar,N. Tiwari,M. Tiwari, M. Lahiri,S.S. Gupta, Part.Part.Syst. Char. 2013, 30, 166-179.
30. S. Plianwong, P. Opanasopit, T. Ngawhirunpat, T. Rojanarata, BioMed Res. Int. 2013, 2013, 9.
31. K.Soda, Y. Kano, T. Nakamura, K. Kasono, M. Kawakami, F. Konishi, J. Immunol. 2005, 175, 237-245.
32. J. Weisell, M.T. Hyvönen, M.R. Häkkinen, N.A. Grigorenko, M. Pietilä, A. Lampinen, S.N. Kochetkov, L. Alhonen, J. Vepsäläinen, T.A. Keinänen, J.Med. Chem. 2010, 53, 5738-5748.
33. K.S. Kumar, V.B. Kumar, P. Paik, J. Nanopart. 2013, 2013, 24.
34. A. Hawe, W. Hulse, W. Jiskoot, R. Forbes, Pharm. Res. 2011, 28, 2302-2310.
35. Y. Wang, S. Gao, W.H. Ye, H.S. Yoon, Y.Y. Yang, Nature mater. 2006, 5, 791-796.
36. J.H. Lee, A.J. Nan, Drug Deliv. 2012, 2012, 17.
37. B. Al-Lazikani, U. Banerji, P. Workman, Nat Biotech. 2012, 30, 679-692.
38. K.E. Uhrich, S.E.M. Ibim, D.R. Larrier, R. Langer, C.T. Laurencin, Biomaterials 1998, 19, 2045-2050.
39. B.Vaisman, D.E.Ickowicz,E.Abtew, M. Haim-Zada, A. Shikanov, A.J. Domb, Biomacromolecules 2013, 14, 1465-1473.
40. S. Zeng, F. Wu, B. Li, X. Song, Y. Zheng, G. He, C. Peng, W. Huang, Scientific World Journal 2014, 2014, 10.
41. G. Su, H. Zhou, Q. Mu, Y. Zhang, L. Li, P. Jiao, G. Jiang, B. Yan, J.Phys. Chem. C 2012, 116 , 4993-4998.
42. R. Chen, S. Khormaee, M.E. Eccleston, N.K.H. Slater, Biomaterials 2009, 30, 1954-1961.
43. B.I.Cerda-Cristerna, H. Flores, A. Pozos-Guillén, E. Pérez, C. Sevrin, C. Grandfils, J. Controlled Rel. 2011, 153, 269-277.
44. R.V. Benjaminsen, M.A. Mattebjerg, J.R. Henriksen, S.M. Moghimi, T.L. Andresen, Mol Ther. 2013, 21 , 149-157.
45. N. Gulati, R. Rastogi, A.K. Dinda, R. Saxena, V. Koul, Colloids Surf., B 2010, 79, 164-173.
46. S.V. Lale, R. G. Aswathy, A. Aravind, D.S. Kumar, V. Koul, Biomacromolecules 2014, 15 (5), 1737-1752.
47. M.F. Ilker, K. Nüsslein, G.N. Tew, E.B. Coughlin, J. Am. Chem. Soc. 2004, 126, 15870-15875.
48. K. Luo, C. Li, L. Li, W. She, G. Wang, Z. Gu, Biomaterials 2012, 33, 4917-4927.